Evidence of PPII-like helical conformation and glass transition in a self-assembled solid-state polypeptide-surfactant complex: Poly(L-histidine)/docylbenzenesulfonic acid

ARTICLE *in* BIOMACROMOLECULES · JUNE 2008

Impact Factor: 5.75 · DOI: 10.1021/bm7012845 · Source: PubMed

Evidence of PPII-like Helical Conformation and Glass Transition in a Self-Assembled Solid-State Polypeptide−Surfactant Complex: Poly(L-histidine)/Docylbenzenesulfonic Acid

Ramasubbu Ramani,[†,‡] Sirkku Hanski,[†] Ari Laiho,[†] Roman Tuma,[§] Simo Kilpeläinen,[||] Filip Tuomisto,[||] Janne Ruokolainen,[†] and Olli Ikkala*[,†]

Laboratory of Molecular Materials, Department of Engineering Physics and Mathematics and Centre for New Materials, Helsinki University of Technology, P.O. Box 5100, FI-02015 TKK, Espoo, Finland, Institute of Biotechnology, University of Helsinki, P.O. Box 65, Viikinkaari 1, FI-00014 Helsinki, Finland, and Laboratory of Physics, Helsinki University of Technology, P.O. Box 1100, FI-02015 TKK, Espoo, Finland

Received November 20, 2007; Revised Manuscript Received February 1, 2008

We present lamellar self-assembly of cationic poly(L-histidine) (PLH) stoichiometrically complexed with an anionic surfactant, dodecyl benzenesulfonic acid (DBSA), which allows a stabilized conformation reminiscent of polyproline type II (PPII) left-handed helices. Such a conformation has no intrapeptide hydrogen bonds, and it has previously been found to be one source of flexibility, e.g., in collagen and elastin, as well as an intermediate in silk processing. PLH(DBSA)$_{1.0}$ complexes were characterized by Fourier transform infrared spectroscopy (FTIR), circular dichroism (CD), small-angle X-ray scattering (SAXS), transmission electron microscopy (TEM), and differential scanning calorimetry (DSC). The PPII-like conformation in PLH(DBSA)$_{1.0}$ is revealed by characteristic CD and FTIR spectra, where the latter indicates absence of intrachain peptide hydrogen bonds. In addition, a glass transition was directly verified by DSC at ca. 135 °C for PLH(DBSA)$_{1.0}$ and indirectly by SAXS and TEM in comparison to pure PLH at 165 °C, thus indicating plasticization. Glass transitions have not been observed before in polypeptide−surfactant complexes. The present results show that surfactant binding can be a simple scheme to provide steric crowding to stabilize PPII conformation to tune the polypeptide properties, plasticization and flexibility.

Introduction

Self-assembly is a powerful approach for fabricating supramolecular structures based on weak and competing interactions.[1–4] In this context, stoichiometric complexes comprising polyelectrolytes and oppositely charged surfactants have attracted considerable interest due to their facile preparation.[5–21] In the solid state, they self-assemble to form polymeric comb-shaped supramolecular architectures, as nonpolar repulsive flexible or mesogenic side chains are linked to the charged polymeric main chain through ionic bonding. Most of the work on solid-state polyelectrolyte−surfactant self-assembly has dealt with synthetic polyelectrolytes and low molecular weight amphiphiles.[5,7–9,15,19,20] Also, polypeptide−surfactant self-assemblies have received considerable interest as peptides can adopt secondary structures, such as α-helices and β-sheets, in addition to random coils.[6,10–12,14,18,21–23] The complexes of poly(α,L-glutamate) form stable α-helical conformation,[11,12] whereas poly(L-lysine) often prefers extended β-sheet conformation.[10,14] The peptide conformations in these complexes, however, depend on, e.g., solvent, processing history, temperature, and pH. Interestingly, a recent study on hyperbranched polylysine reveals that its secondary structure was suppressed because of its branched nature.[24] More recently, even hierarchical self-assembly in solid state has been reported in diblock copolypeptides as well as in peptide−synthetic polymer hybrid block copolymers by ionic bonding of the surfactants to one of the blocks.[25,26]

Poly(L-histidine) (PLH) contains an imidazole group in the side chain, which can mediate proton transfer in enzymatic catalysis and is important for metal coordination in proteins.[27,28] In solid state the complexation of PLH has been studied with retinoic acid[16] and dodecanoic acid[18] to form nanoparticles for drug delivery purposes. Also a layer-by-layer complexation with poly(styrene sulfonate)[29] in solid state has been reported.

The research herein focuses on the structure and properties of self-assembled stoichiometric complexes between PLH and an anionic surfactant, dodecylbenzenesulfonic acid (DBSA) in the solid state. Two novel features are reported. (1) This is the first polypeptide−surfactant self-assembled complex with the polypeptide adapting to polyproline type II (PPII) helical conformation. (2) For the first time, we show the presence of a glass transition temperature (T_g) in a polypeptide−surfactant complex. Not surprisingly, this complex forms a lamellar self-assembled structure according to small-angle X-ray scattering (SAXS) and transmission electron microscopy (TEM). Circular dichroism (CD) and Fourier transform infrared (FTIR) spectroscopy show the characteristics of PPII helices. This secondary structure is not stabilized by intrapeptide hydrogen bonds, unlike the more conventional α-helices. Beyond polyproline, the PPII helical conformation has been observed in a number of other polypeptide systems. Importantly, we point out that creation and stabilization of PPII conformation has aroused considerable recent interest: It is observed in silk protein aqueous solution before spinning and it is expected to have a role in the spinning

* Corresponding author: olli.ikkala@tkk.fi.
[†] Laboratory of Molecular Materials, Department of Engineering Physics and Mathematics and Centre for New Materials, Helsinki University of Technology.
[‡] Permanent address: Polymer Science Division, DMSRDE, G.T. Road, Kanpur 208 013, India.
[§] Institute of Biotechnology, University of Helsinki.
[||] Laboratory of Physics, Helsinki University of Technology.

10.1021/bm7012845 CCC: $40.75
Published on Web 04/18/2008

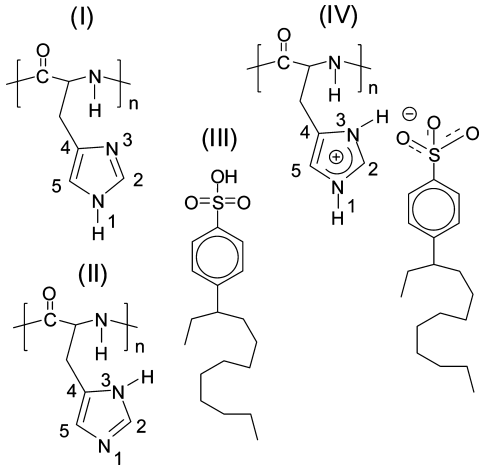

Figure 1. Chemical formulas of the materials used in this work. Two tautomeric forms of PLH are shown (I and II). The DBSA is depicted in one of its possible branched alkyl tail structures (III), and the ionic complex is illustrated in (IV).

process, and it provides flexibility to elastic proteins, such as collagen and elastin.[30–32] Furthermore, the T_g is revealed from the "frozen-in" disorder effect in the glassy state upon treating this complex with chloroform and formation of highly ordered lamellar structure after a short thermal annealing above T_g, as shown by SAXS and TEM.

Experimental Section

Materials. Poly(L-histidine) (M_w = 9850 g mol^{-1}, DP = 72) was used as received from Sigma Chemicals. Dodecylbenzenesulfonic acid soft type (DBSA) having a branched alkyl tail was purchased from Tokyo Kasei, Japan. A branched alkyl tail suppresses the side chain crystalline packing upon complexation. Chloroform (Aldrich) of the highest purity available was used as received. Ultrapure water (MilliQ) from a Millipore system was used to prepare all the aqueous solutions.

Preparation of PLH(DBSA)$_{1.0}$. Complexation between DBSA and PLH can take place if the proton is transferred from the acidic DBSA to the basic PLH. The stoichiometric complex PLH(DBSA)$_{1.0}$ contains one DBSA molecule ionically bonded to each imidazole group of the PLH repeat units. The complex was prepared by precipitation from aqueous solutions: The PLH dissolves in water under acidic conditions (when pH is maintained slightly below 3) as the acidity improves solubility due to the protonation. Hence, raising the pH of the solution would help to form the complex between the acidic DBSA and PLH. For this reason, PLH was first dissolved in water and the concentration was adjusted to 1 wt %, where pH <3 was set by 1 M HCl addition. Thereafter, the pH was adjusted to 5.5 by dropwise addition of 1 M NaOH to increase the binding efficiency toward acidic DBSA. Subsequently, such a solution was used to prepare PLH films, unless otherwise stated. Aqueous solution of DBSA (1.0 wt %) was prepared separately. Equimolar quantities of the two solutions were combined, leading to immediate precipitation, but they were mixed with a rotator additionally for ∼24 h to ensure complete complexation. The resulting precipitate was thoroughly washed four times with water to remove traces of NaCl. The $AgNO_3$ test was performed on the final decanted solution and was tested negative for Cl^- ions. The resulting precipitate was air-dried for at least 24 h and then dried in vacuum at 30 °C for 48 h (subsequently denoted as PLH(DBSA)$_{1.0}^{aq}$). Elemental analysis showed a good agreement between the experimental and calculated weight fractions of C, N, and H (C, 61.1_{exp} (62.2_{calc}); N, 8.9_{exp} (9.1_{calc}); H, 8.5_{exp} (8.1_{calc})), which justifies to denote the complex as stoichiometric PLH(DBSA)$_{1.0}$. Figure 1 shows the starting materials as well as the stoichiometric complex.

Chloroform Treatment of PLH(DBSA)$_{1.0}$. In order to study the possible conformational and structural changes of the complex due to organic solvent dissolution and drying step, the precipitated and dried PLH(DBSA)$_{1.0}$ powder was dissolved in chloroform (1.0 wt%), which rendered a film upon slow solvent evaporation during several hours, followed by vacuum drying for ∼24 h (subsequently denoted as PLH(DBSA)$_{1.0}^{CHCl_3}$). This step was also relevant for, e.g., CD measurements.

Characterization methods. *Fourier Transform Infrared Spectroscopy (FTIR).* The pure PLH and aqueous precipitated PLH(DBSA)$_{1.0}$ complexes were mixed with KBr in a mortar and pressed to pellets. On the other hand, pure DBSA and PLH(DBSA)$_{1.0}^{CHCl_3}$ films were cast from chloroform on KBr tablets and dried in vacuum for at least 24 h. Infrared spectra were recorded using a Nicolet 380 FTIR spectrometer. Sixty-four scans were recorded and averaged with a resolution of 2 cm^{-1}.

Circular Dichroism (CD). Films were cast from chloroform on a quartz window and dried in vacuum for at least 24 h. Circular dichroism measurements were performed with a JASCO J-715 CD spectropolarimeter using a scanning speed of 50 nm/min. The CD spectra were recorded with 1 nm bandwidth and 0.5 nm step resolution, and the mean residue ellipticity was determined. Each spectrum is an average of five individual scans. To obtain good quality spectrum, CD spectra were acquired for different film thicknesses. Then the optimum thickness was selected and the spectra were acquired in different orientations at room temperature. The best of the room temperature spectra was chosen for an annealing study and the same has been reported. The sample on quartz substrate was heated at a heating rate of 5 °C/min using a microprocessor-controlled heating system.

Small-Angle X-ray Scattering (SAXS). The samples were sealed between two thin Kapton foils. The SAXS system consists of a two-dimensional area detector (Bruker AXS) and a Bruker MICROSTAR rotating anode X-ray source with Montel optics (Cu Kα radiation, λ = 1.54 Å). The beam was further collimated with four sets of four-blade slits resulting in a beam of about 1 mm × 1 mm at the sample position. A distance of ∼0.45 m was maintained between the sample and the detector. The magnitude of the scattering vector is given by $q = (4\pi/\lambda) \sin \theta$, where 2θ is the scattering angle. The q range was calibrated with silver behenate standard.

Transmission Electron Microscopy (TEM). The epoxy embedded bulk samples were cryomicrotomed at −60 °C using a Leica Ultracut UCT ultramicrotome and a diamond knife to yield sections 50–60 nm in thickness. Dry sections were placed on a 600 mesh copper grid and stained with ruthenium tetroxide (RuO_4) for ∼20 min for contrast enhancement. Bright field TEM was performed on a FEI Tecnai 12 transmission electron microscope operating at an accelerating voltage of 120 kV.

Differential Scanning Calorimetry (DSC). Thermal transitions of PLH(DBSA)$_{1.0}$ complexes (mass ∼5 mg) were measured using a Mettler DSC-821. The heating/cooling scans were performed with a heating/ cooling rate of 10 °C/min, and a nitrogen purge flow of 80 ml/min was used. Samples were not exposed to temperatures above 230 °C to avoid possible thermal degradation. The glass transition was calculated at the midpoint of the slope change during the third and fourth heating traces.

Results and Discussion

In the following, we will discuss the stoichiometric ionic complexation of poly(L-histidine) with branched alkyl tail surfactant DBSA, the effect of organic solvent treatment on the secondary structure and self-assembly, as well as the thermal behavior and the effects of glass transition therein.

We will first discuss formation of the ionic complex. As expected, the complexation most readily manifests as a precipitation when stoichiometric amounts of aqueous solutions of PLH and DBSA are combined. FTIR measurements give further insight to the complexation shown in the parts A−C of Figure 2. For pure PLH we observe two bands assigned to the

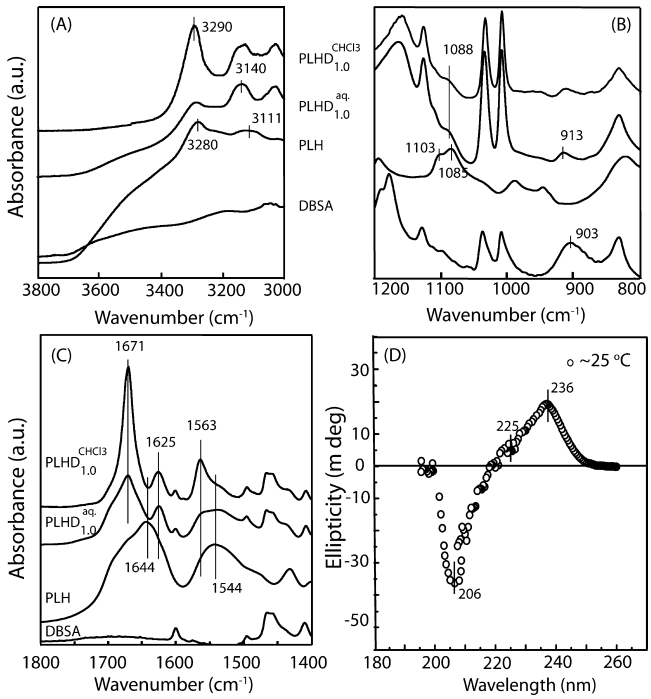

Figure 2. FTIR spectra for PLH, DBSA, and solid-state PLH(DBSA)$_{1.0}$ after precipitation from aqueous solution (PLH(DBSA)$_{1.0}^{aq}$) and after further chloroform treatment (PLH(DBSA)$_{1.0}^{CHCl_3}$): (A) amide A bands; (B) 1200–800 cm^{-1} bands relevant for the imidazole group; (C) amide I and II bands; (D) CD spectrum at room temperature for PLH(DBSA)$_{1.0}^{CHCl_3}$ film after chloroform casting. PLHD$_{1.0}$ denotes PLH(DBSA)$_{1.0}$.

imidazole C5N1 stretchings at 1085 and 1103 cm^{-1} (Figure 2B), as expected for the two tautomeric forms I and II (see Figure 1).[33] With equimolar DBSA addition, the C5N1 stretch leads to a peak at ca. 1088 cm^{-1} (Figure 2B), indicating protonated imidazole groups.[29,33] The protonation of the imidazole group is even more clearly evidenced by the formation of a new band at ca. 1625 cm^{-1} (Figure 2C), which is due to ring stretch (mainly C4−C5 stretch) of the protonated imidazole.[29,33] In addition, the NH stretching peak of the imidazole ring for pure PLH at ca. 3111 cm^{-1} shifts to 3140 cm^{-1} with an increase in peak intensity (Figure 2A). This agrees with the results of poly(4,5-vinyl imidazole) protonated with phosphoric acid, where a corresponding NH shift of 30 cm^{-1} and an increased peak intensity indicate complete protonation of the imidazole group.[34] Furthermore, the pure DBSA exhibits a band at ca. 900 cm^{-1} due to $-SO_3H$ absorption,[9] which completely disappears for the prepared complex, suggesting that essentially no DBSA remains in an acidic form in the complex (Figure 2B). These observations show spectroscopically that the complex between PLH and DBSA takes place. As described in the Experimental Section, elemental analysis demonstrates a stoichiometric complex between PLH and DBSA within the experimental resolution. We thus denote the resulting complex as PLH(DBSA)$_{1.0}$.

Next it turns out instructive to discuss the secondary structures based on CD spectroscopy, before presenting the other relevant FTIR bands. Pure PLH and aqueous precipitated PLH(DBSA)$_{1.0}^{aq}$ did not allow CD spectroscopy, as they remained in powder form. But casting the complex from chloroform (PLH(DBSA)$_{1.0}^{CHCl_3}$) allowed high quality films, and Figure 2D presents the CD spectrum of such a film recorded in the far-UV region (195–260 nm) at room temperature (~25 °C). The spectrum displays a strong negative band at ca. 206 nm, a strong positive band centered at ca. 236 nm with, importantly, a positive shoulder at ca. 225 nm, a cross-over near 220 nm, and the ellipticity close to zero near 200 nm. This shape is uncommon and excludes the classical polypeptide secondary structures, such as α-helix, β-sheet, and random coil (see Supporting Information for CD spectra of pure PLH solution in β-sheet and random coil conformations). Instead, the spectral shape shows the characteristic features of polyproline type II (PPII) secondary structure: PPII is a left-handed helix with three residues per turn, where all peptide bonds are in trans configuration with no intramolecular peptide hydrogen bonds, and the rise per residue is 3.1 Å.[35,36] It is relevant within the present context that it minimizes the contacts between the side chains; i.e., it is stabilized by steric reasons. PPII was originally found in polyproline, but the more recent literature describes that it is observed also in several other polypeptides and in short protein segments, and it can have an important role, e.g., in the silk processing and providing elasticity in collagen and elastin.[30–32,37,38] The CD spectrum of PPII characteristically shows a strong negative band at 202–206 nm and a weak positive band at 220–226 nm, and sometimes ellipticity close to zero at 200 nm.[31,35,36] Therefore, the spectral shape is strikingly similar to that of the chloroform cast PLH(DBSA)$_{1.0}^{CHCl_3}$. In PLH(DBSA)$_{1.0}^{CHCl_3}$ the absorption at 236 nm is at too long a wavelength to be assigned directly to polypeptide conformation, and therefore, it is suggested to be a contribution from the imidazole group of PLH.[39,40] In fact, superimposed CD absorption at higher wavelengths has been observed in the case of PPII conformations if aromatic side chains are contained.[31] In conclusion, CD spectroscopy suggests that the secondary structure of PLH(DBSA)$_{1.0}^{CHCl_3}$ is essentially PPII-like.

FTIR spectroscopy provides a way to study peptide–peptide hydrogen bonds in order to get further support for the PPII-like conformation. The amide I band at 1700–1600 cm^{-1} is characteristic to the peptide C═O stretching and reveals the information whether the carbonyl groups participate in the hydrogen bonding or not. The pure PLH film cast from aqueous solution (pH 5.5) shows broad amide I band at ca. 1644 cm^{-1} (Figure 2C). By contrast, in PLH(DBSA)$_{1.0}$ the amide I band is shifted to 1671 cm^{-1}, i.e., to considerably higher frequencies. This band is distinct for the aqueous precipitated PLH(DBSA)$_{1.0}^{aq}$ but becomes even narrower after chloroform treatment. Note that several types of polymers exhibit the amide I band in the range 1680–1670 cm^{-1} in the absence of hydrogen bonding.[41] Therefore, we suggest that the upshifted amide I band at 1671 cm^{-1} in PLH(DBSA)$_{1.0}$ in comparison to that of pure PLH at 1644 cm^{-1} indicates that the peptide carbonyl groups become essentially free from hydrogen bonding upon complexation of the polypeptide with DBSA. The frequency upshift can be explained by the increase in the double bond character of the carbonyl group in the absence of hydrogen bonding, i.e., a decreased electronegative character of the oxygen atom.[42] In fact, the presence of a strong amide I band at 1672–1670 cm^{-1} in short peptide sequences in the solid state has been reported to be a IR diagnostic marker for PPII helices.[43,44] In conclusion, the FTIR results are in agreement with the CD spectroscopy, implying that the conformation of PLH(DBSA)$_{1.0}^{CHCl_3}$ is PPII-like, where the peptide carbonyls do not essentially act as hydrogen bonding acceptors. The PPII-like secondary structure is easy to accept, as this conformation allows the steric crowding effect of the relatively bulky side chains in PLH(DBSA)$_{1.0}$ to be minimized. In the case of PLH(DBSA)$_{1.0}^{aq}$ the lack of direct CD spectra (as explained before) does not allow definite conclusion of the PPII conformation. However, as FTIR and

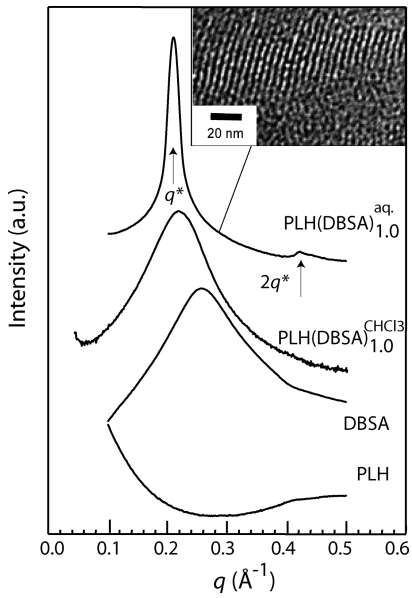

Figure 3. SAXS profiles of PLH (pH 5.5), DBSA, $PLH(DBSA)_{1.0}^{CHCl_3}$ (complex cast from chloroform), and $PLH(DBSA)_{1.0}^{aq}$ (precipitated from aqueous solution). Note that the intensity is in a logarithmic scale. The inset represents a transmission electron micrograph of $PLH(DBSA)_{1.0}^{aq}$ at ~25 °C showing a well-defined lamellar structure.

other properties of the precipitated complex show that it behaves in many respects similar to the chloroform-cast sample, we expect that its conformation also is PPII-like, even if the actual degree of order can be slightly different.

Furthermore, hydrogen bonds of the peptide amines can be studied based on the FTIR amide II band at 1580−1500 cm^{-1}, which is characteristic to both C−N stretching and N−H in-plane bending. PLH film cast from aqueous solution (pH 5.5) shows a broad amide II band at ca. 1544 cm^{-1} (Figure 2C). In $PLH(DBSA)_{1.0}$ the amide II band undergoes a change, as a new peak is observed at 1563 cm^{-1} in addition to the reduced absorption at 1544 cm^{-1}. The absorption at 1563 cm^{-1} becomes more distinct after chloroform treatment. The shift of the amide II band to higher frequencies, as DBSA is added, suggests the presence of hydrogen bonds of the amide NH groups in the $PLH(DBSA)_{1.0}$. As we have shown above that in $PLH(DBSA)_{1.0}$ the peptide carbonyls do not essentially take part in hydrogen bonding, the only available acceptor sites for strong hydrogen bonding are the oxygens of the sulfonate anions in the ionically complexed DBSA. Therefore, we suggest that new hydrogen bonds are formed between the backbone peptide amines and DBSA sulfonates; see later Figure 8A. Such a hydrogen bonding of NH with the sulfonate oxygens leaving backbone C═O groups free from hydrogen bonding is in agreement with the PPII-like structure. Related surfactant binding has been reported recently for poly(γ-glutamic) acid complexed with dodecyltrimethylammonium surfactant.[21] Also the intense and narrow amide A band at 3290 cm^{-1} (Figure 2A) indicates strong hydrogen bonding at the polypeptide amine site.

We next studied the room temperature self-assembly of $PLH(DBSA)_{1.0}$; see Figure 3 for the SAXS and TEM results. Pure PLH does not show any structure at this length scale. This is in agreement with FTIR, which shows broad peaks characteristic to poorly ordered material (see Figure 2A−C). DBSA exhibits only a very broad scattering peak at $q = 0.266$ $Å^{-1}$. Instead, $PLH(DBSA)_{1.0}^{aq}$ precipitated from aqueous solution shows a sharp, intense reflection at $q^* = 0.215$ $Å^{-1}$ (first order reflection) accompanied by a weaker but still clear second-order reflection at $2q^*$, consistent with a lamellar self-assembly with a periodicity of ca. 29.2 Å. Complexations of oppositely charged surfactants with polypeptides like poly(L-lysine) and poly(α,L-glutamate) have been reported to form lamellar structures in agreement with our results.[10−14] A TEM micrograph for $PLH(DBSA)_{1.0}^{aq}$ is presented as an inset in Figure 3. The black areas represent the polar PLH and surfactant head domains and white areas are nonpolar alkyl tail layers, which repel the charged backbone. The TEM micrograph confirms the well-ordered lamellar structure of $PLH(DBSA)_{1.0}^{aq}$ with a periodicity of ca. 36 Å, which is a bit higher than the value obtained from SAXS results. The cutting compression effect during sectioning could be a possible reason for this difference in periodicity. In passing, it can be stated that the wide-angle X-ray scattering (WAXS) of $PLH(DBSA)_{1.0}^{aq}$ in the q range 0.3−2.5 $Å^{-1}$ exhibits only a broad halo showing the absence of any crystalline structure (data not shown).

The SAXS curve of the $PLH(DBSA)_{1.0}^{CHCl_3}$ film at room temperature (Figure 3) is surprisingly different in comparison to that of $PLH(DBSA)_{1.0}^{aq}$. Instead of the high-intensity first-order reflection of the latter one, the chloroform-cast sample shows only a broad peak at $q = 0.215$ $Å^{-1}$ with no trace of a second-order reflection. In fact, the shape resembles disordered structures just beyond the order–disorder transitions in polymer−amphiphile complexes or block copolymers.[45] The broad reflection is surprising, as one could have expected better "solvent-annealed" structures after organic solvent treatment in contrast to the structures formed rapidly in the process of aqueous precipitation, as also the amide I and II bands in FTIR (Figure 2C) showed narrow absorption peaks for $PLH(DBSA)_{1.0}^{CHCl_3}$. TEM (Figure 4C), in fact, does show some order for $PLH(DBSA)_{1.0}^{CHCl_3}$ at room temperature but with poor long-range order and a large number of defects. This is consistent with the SAXS with only a broad reflection. Similar to the aqueous precipitated sample, the WAXS profile of $PLH(DBSA)_{1.0}^{CHCl_3}$ in the q range 0.3−2.5 $Å^{-1}$ shows only a broad halo due to absence of any crystalline structure (data not shown).

Puzzled with the poor ordering of the chloroform-treated $PLH(DBSA)_{1.0}^{CHCl_3}$, we next studied the effect of heating on the self-assembly using SAXS and TEM. Figure 4 shows the SAXS curves for $PLH(DBSA)_{1.0}^{aq}$ (A) and $PLH(DBSA)_{1.0}^{CHCl_3}$ (B) upon heating and cooling. The aqueous precipitated sample shows essentially no change in SAXS upon heating to 220 °C, except a small shift of the peak positions to larger scattering angles upon cooling back to room temperature and a slight increase in the intensity of the second-order reflection. In the chloroform-treated sample, the broad peak observed at room temperature gets narrower on heating past 160 °C and gains intensity and the second-order reflection appears indicating a lamellar structure, similar to the one obtained for the aqueous sample. The so-formed lamellar structure remains upon cooling. The change from poorly ordered structure with short-range order to well-ordered lamellar structure upon heating is observed also using TEM (Figure 4C,D).

The effects of heating on the $PLH(DBSA)_{1.0}$ shows also in FTIR and CD spectroscopy. In agreement with SAXS, the heating of $PLH(DBSA)_{1.0}^{aq}$ up to 190 °C showed no significant spectral changes in FTIR (data not shown), indicating no changes in the secondary structure. But for $PLH(DBSA)_{1.0}^{CHCl_3}$, clear changes were observed both in FTIR (Figure 5) and in CD (Figure 6), as the temperature was increased. Upon heating up to ca. 120 °C, the intensities of the amide A band at 3290

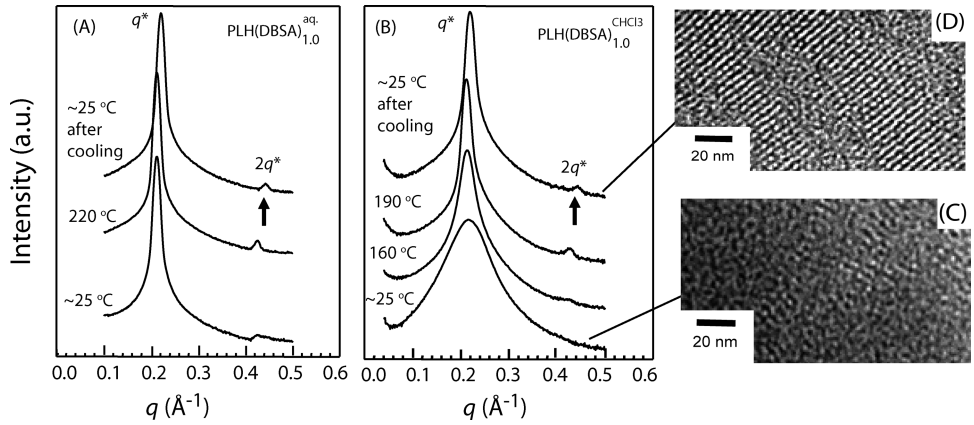

Figure 4. SAXS profiles of $PLH(DBSA)_{1.0}$ as precipitated from aqueous solution (A) and after casting from chloroform (B) upon heating and subsequent cooling. Note that the intensity is in a logarithmic scale. Transmission electron micrographs of $PLH(DBSA)_{1.0}{}^{CHCl_3}$ at room temperature (C) and when heated to 190 °C and cooled back to room temperature (D).

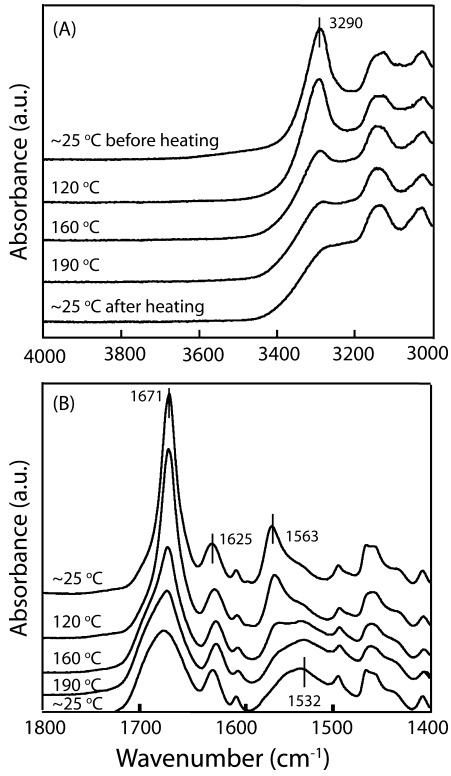

Figure 5. FTIR absorption spectra of $PLH(DBSA)_{1.0}{}^{CHCl_3}$ film before heating (top curves), upon heating, and after cooling back to room temperature (bottom curves) for bands (A) 4000–3000 cm^{-1} and (B) 1800–1400 cm^{-1}.

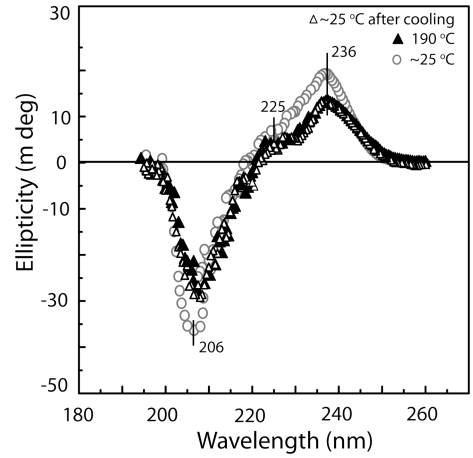

Figure 6. CD spectra of $PLH(DBSA)_{1.0}{}^{CHCl_3}$ film at room temperature before heating (gray open circles, shown already in Figure 2, here as a reference), at 190 °C (closed triangles), and at room temperature after cooling (open triangles).

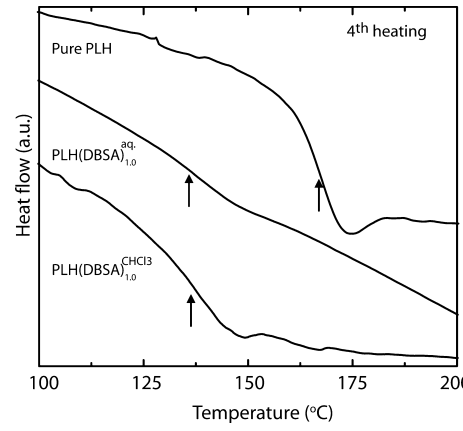

Figure 7. The DSC curves for the fourth heating at 10 °C/min for pristine PLH, $PLH(DBSA)_{1.0}{}^{aq}$ precipitated from aqueous solution, and $PLH(DBSA)_{1.0}{}^{CHCl_3}$ cast from chloroform.

cm^{-1} (probing the peptide amines) and amide I band at 1671 cm^{-1} (probing the peptide carbonyls) decrease only slightly, but passing ca. 160 °C an abrupt and irreversible decrease in the intensities is observed (Figure 5). In parallel, within the amide II band at 1544 cm^{-1} (probing the peptide amines), a lower frequency shoulder develops at 1532 cm^{-1} when passing ca. 120 °C, and it becomes the dominant amide II peak at 160 °C. No significant further changes are observed in amide A and II bands upon heating from 160 to 190 °C and upon subsequent cooling to room temperature. These results suggest the disappearance of hydrogen bonds between the backbone NH groups and the sulfonate oxygens after passing ca. 160 °C in $PLH(DBSA)_{1.0}{}^{CHCl_3}$ (see Figure 8B). There are no significant changes in these amide bands upon subsequent heatings, but the phenomenon is totally reversible upon recasting the film from chloroform solution (data not shown).

Furthermore, an irreversible decrease in amide I band intensity points to an additional interesting feature. In a recent FTIR study on heat-induced changes in a short helical protein, villin headpiece helical subdomain (HP36), the authors observed a decrease in intensity of the amide I band near 1674 cm^{-1} upon heating and explained this change as due to melting of turn regions.[46] In the present case, the decrease in intensity of the amide I band might be taken as due to the slight loss of helical

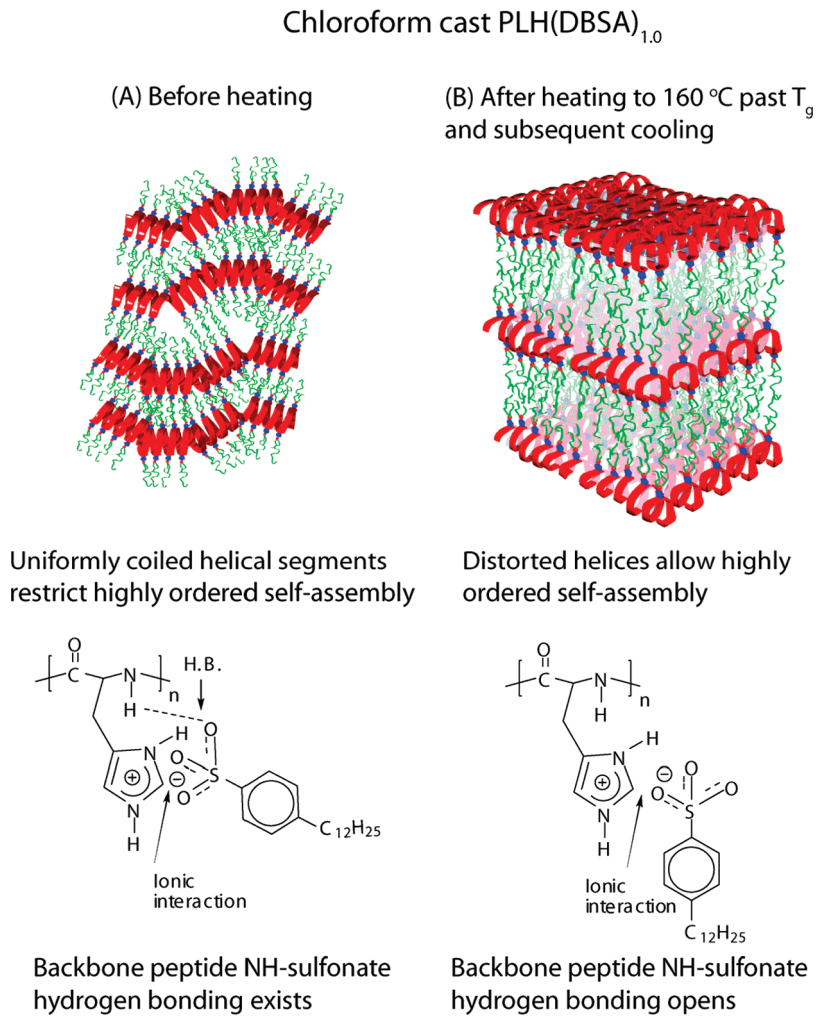

Figure 8. Schematic representation of the proposed ionic complexation between PLH and DBSA, which leads to PPII-like helices with physically bound surfactants, as well as the lamellar structure for the PLH(DBSA)$_{1.0}^{CHCl_3}$ film before and after heating it to past ca.160 °C, i.e., past the glass transition. The scheme shows the suggested additional hydrogen bonds between the peptide amines and sulfonate oxygens as formed in the chloroform casting and released by heating past glass transition.

turns upon heating (see also CD data in the next paragraph). Stretching of helical chains along the long axis and associated changes in its structure are the most possible heat-induced changes which could lead to this effect. In an earlier work on the complexes of poly(α,L-glutamate) with cationic surfactants in which the peptide was in α-helical conformation, heat treatment shifted the amide I band to a higher frequency and the amide II band to a lower frequency.[12] These changes were explained as due to a temperature-induced weakening and disruption of intramolecular hydrogen bonds, which is in agreement with our interpretation.

Figure 6 presents the CD spectra of PLH(DBSA)$_{1.0}^{CHCl_3}$ film in the far-UV region (195–260 nm) at 190 °C (solid triangles), at the room temperature after cooling (open triangles), and at the room temperature before heating (gray open circles, reproduced from Figure 2D to facilitate comparison). When heated to 190 °C and subsequently cooled, the characteristics of PPII secondary structure are conserved. Still changes are observed, as the bands at 206 and 236 nm are slightly reduced, whereas the shoulder at 225 nm becomes more pronounced. The decrease in the prominent negative band intensity at 206 nm suggests some loss of the PPII helicity, consistent with earlier work on PPII-rich peptides[38] as well as our FTIR results with the amide I band at 1671 cm^{-1} showing a decrease in intensity on passing ca. 160 °C. The observed CD spectral changes also irreversibly remain upon subsequent cooling. In conclusion, the CD spectroscopy in combination with FTIR suggests that at room temperature, the chloroform cast PLH(DBSA)$_{1.0}^{CHCl_3}$ adapts a relatively well-defined PPII-like helical conformation, which undergoes an irreversible change upon heating past ca. 160 °C to less-well-defined PPII-like helical conformation.

The SAXS, TEM, FTIR, and CD spectroscopy of PLH-(DBSA)$_{1.0}^{CHCl_3}$ indicate that an irreversible transition takes place near 160 °C upon heating. Therefore DSC measurements were performed to PLH(DBSA)$_{1.0}$ after the aqueous precipitation and after subsequent chloroform treatment in an effort to explore the possible existence of a glass transition near that temperature. But, neither PLH(DBSA)$_{1.0}^{aq}$ nor PLH(DBSA)$_{1.0}^{CHCl_3}$ showed any signs of a glass transition upon the first heating–cooling cycle. However, the literature indicates that a glass transition can become observable after a repeated thermal cycling: For example, solid-state complexes of polypeptides with metal chlorides allowed identification of T_g using DSC only after the third and fourth heating cycles.[47,48] Accordingly, we performed DSC measurements up to four heating–cooling cycles and this allowed to observe quite consistent signatures of glass transition (Figure 7). The T_g of pristine PLH is observed at 165 °C and is comparable to 169 °C reported in the literature.[47] The T_g for

$PLH(DBSA)_{1.0}^{aq}$ is observed at ca. 133 °C and an almost identical value ca. 135 °C is obtained for $PLH(DBSA)_{1.0}^{CHCl_3}$ film.

The structural behavior observed with CD, FTIR, TEM, and SAXS for $PLH(DBSA)_{1.0}^{CHCl_3}$ are summarized in Figure 8. At room temperature the CD and FTIR measurements indicate a well-defined PPII-like helical secondary structure with no peptide–peptide hydrogen bonds. The surfactant sulfonates form hydrogen bonds with the peptide amine groups in PLH, whereas the peptide carbonyls are essentially free from hydrogen bonds. Surprisingly, despite the well-ordered secondary structure of $PLH(DBSA)_{1.0}^{CHCl_3}$, the self-assembled order is poor at room temperature based on SAXS and TEM. We suggest that at room temperature the ionically complexed surfactants having additional hydrogen bonding with the backbone amines pose a steric hindrance to allow a proper packing of the helices. Such additional hydrogen bonds can be effects of "frozen-in" disorder due to the chloroform casting, as chloroform is a well-known solvent to promote hydrogen bonds. Upon heating, clear changes take place when passing the glass transition temperature for the $PLH(DBSA)_{1.0}^{CHCl_3}$ complex. The suppression of the amide A peak at 3290 cm^{-1} as well as the broadening of the amide II peak in FTIR indicate that the peptide amines become less efficient hydrogen-bond donors upon heating past the glass transition, and the hydrogen bonds between them and sulfonates open by the thermal agitation (Figure 8B). This may release steric hindrances to allow improved self-assembled order, as observed by SAXS and TEM. But when the sample is heated, FTIR spectra show a decrease of amide I band at 1671 cm^{-1}, which suggests that the helicity is less regular, in accordance with the CD results that show a reduced negative minimum at 206 nm. When the sample is again cooled, the changes in the self-assembly and conformation remain. Upon recasting the film from chloroform, the helicity is almost regained as observed in the amide I band intensity, which leads to poor lamellar structure (data not shown). Therefore, the results suggest that well-defined PPII-like helicity and well-defined lamellar self-assembly are not fully compatible in the present system and that lamellar self-assembly is improved at the cost of more perfect helicity. Before chloroform treatment, for $PLH(DBSA)_{1.0}^{aq}$, the FTIR measurements suggest poorer PPII-like helicity, which enables well-defined lamellar self-assembly. This structure is stable at all measured temperatures.

Conclusions

We have shown that poly(L-histidine) stoichiometrically complexed with soft type dodecylbenzenesulfonic acid, i.e., $PLH(DBSA)_{1.0}$, forms a lamellar self-assembled structure with the polypeptide backbone adapting a PPII-like helical structure in contrast to more conventional conformations. The left-handed PPII-helix is a source for flexibility in several proteins, like collagen and elastin, and an intermediate, e.g., in silk spinning. The present work shows that PPII-like conformation can be stabilized by surfactant binding due to steric reasons to reduce the side chain interactions. Also the absence of backbone hydrogen bonds is expected to ease the process of designing future novel functional biomaterials akin to synthetic polymers. Further, this work unequivocally proves the existence of a glass transition temperature and plasticization for the first time in a stoichiometric polypeptide−surfactant complex.

Acknowledgment. We thank Panu Hiekkataipale for assistance in SAXS measurements. We gratefully acknowledge Ulla Vainio and Professor Ritva Serimaa of Helsinki University for WAXS measurements. The Laboratory of Polymer Technology of Helsinki University of Technology is acknowledged for providing the DSC. Olli Lehtonen is thanked for the fruitful discussions on molecular modeling. We also thank the NOKIA Research Center for a grant and Dr. Markku Heino for discussions. This work was carried out in the Centre of Excellence of Academy of Finland ("Bio- and Nanopolymers Research Group", 77317).

Supporting Information Available. FTIR data, CD data for aqueous PLH solution at pH 2.5 and 5.5, and polarized optical microscopy images for $PLH(DBSA)_{1.0}^{aq}$ at ~25 °C and at 220 °C as well as for $PLH(DBSA)_{1.0}^{CHCl_3}$ at 160 °C. This material is available free of charge via the Internet at http://pubs.acs.org.

References and Notes

(1) Whitesides, G. M.; Mathias, J. P.; Seto, C. T. *Science* **1991**, *254*, 1312.
(2) Muthukumar, M.; Ober, C. K.; Thomas, E. L. *Science* **1997**, *277*, 1225.
(3) Hamley, I. W. *The Physics of Block Copolymers*; Oxford University Press: Oxford, 1998.
(4) Ikkala, O.; ten Brinke, G. *Science* **2002**, *295*, 2407.
(5) Wegner, G. *Makromol. Chem., Macromol. Symp.* **1986**, *1*, 151.
(6) Goddard, E. D.; Ananthapadmanabhan, K. P. *Interactions of Surfactants with Polymers and Proteins*; CRC Press: Boca Raton, FL, 1993.
(7) Antonietti, M.; Conrad, J.; Thünemann, A. *Macromolecules* **1994**, *27*, 6007.
(8) Zheng, W.-Y.; Wang, R.-H.; Levon, K.; Rong, Z. Y.; Taka, T.; Pan, W. *Makromol. Chem. Phys.* **1995**, *196*, 2443.
(9) Ikkala, O.; Ruokolainen, J.; ten Brinke, G.; Torkkeli, M.; Serimaa, R. *Macromolecules* **1995**, *28*, 7088.
(10) Ponomarenko, E. A.; Tirrell, D. A.; MacKnight, W. J. *Macromolecules* **1996**, *29*, 8751.
(11) Ponomarenko, E. A.; Waddon, A. J.; Tirrell, D. A.; MacKnight, W. J. *Langmuir* **1996**, *12*, 2169.
(12) Ponomarenko, E. A.; Waddon, A. J.; Bakeev, K. N.; Tirrell, D. A.; MacKnight, W. J. *Macromolecules* **1996**, *29*, 4340.
(13) Wenzel, A.; Antonietti, M. *Adv. Mater.* **1997**, *9*, 487.
(14) Ponomarenko, E. A.; Tirrell, D. A.; MacKnight, W. J. *Macromolecules* **1998**, *31*, 1584.
(15) Chen, H.-L.; Hsiao, M.-S. *Macromolecules* **1999**, *32*, 2967.
(16) Thünemann, A. F.; Beyermann, J.; von Ferber, C.; Löwen, H. *Langmuir* **2000**, *16*, 850.
(17) Zhou, S.; Chu, B. *Adv. Mater.* **2000**, *12*, 545.
(18) General, S.; Thünemann, A. F. *Int. J. Pharm.* **2001**, *230*, 11.
(19) Dufour, B.; Rannou, P.; Djurado, D.; Janeczek, H.; Zagorska, M.; de Gayer, A.; Travers, J.-P.; Pron, A. *Chem. Mater.* **2003**, *15*, 1587.
(20) Ganeva, D.; Antonietti, M.; Faul, C. F. J.; Sanderson, R. *Langmuir* **2003**, *19*, 6561.
(21) Zanuy, D.; Alemán, C. *Biomacromolecules* **2007**, *8*, 663.
(22) Branden, C.; Tooze, J. *Introduction to Protein Structure*, 2nd ed.; Garland Publishing: New York, 1999.
(23) Hanski, S.; Junnila, S.; Almásy, L.; Ruokolainen, J.; Ikkala, O. *Macromolecules* **2008**, *41*, 866.
(24) Canilho, N.; Scholl, M.; Klok, H.-A.; Mezzenga, R. *Macromolecules* **2007**, *40*, 8374.
(25) Hanski, S.; Houbenov, N.; Ruokolainen, J.; Chondronicola, D.; Iatrou, H.; Hadjichristidis, N.; Ikkala, O. *Biomacromolecules* **2006**, *7*, 3379.
(26) Hammond, M. R.; Klok, H.-A.; Mezzenga, R. *Macromol. Rapid Commun.* **2008**, *29*, 299.
(27) Sundberg, R. J.; Martin, R. B. *Chem. Rev.* **1974**, *74*, 471.
(28) Marzotto, A.; Nicolini, M.; Braga, F.; Pinto, G. *Inorg. Chim. Acta* **1979**, *34*, L295.
(29) Barreira, S. V. P.; García-Morales, V.; Pereira, C. M.; Manzanares, J. A.; Silva, F. *J. Phys. Chem. B* **2004**, *108*, 17973.
(30) Adzhubei, A. A.; Sternberg, M. J. E. *J. Mol. Biol.* **1993**, *229*, 472.
(31) Bochicchio, B.; Tamburro, A. M. *Chirality* **2002**, *14*, 782.
(32) Lefèvre, T.; Leclerc, J.; Rioux-Dube, J.-F.; Buffeteau, T.; Paquin, M.-C.; Rousseau, M.-E.; Cloutier, I.; Auger, M.; Gagné, S. M.; Boudreault, S.; Cloutier, C.; Pézolet, M. *Biomacromolecules* **2007**, *8*, 2342.
(33) Hasegawa, K.; Ono, T.; Noguchi, T. *J. Phys. Chem. B* **2000**, *104*, 4253.
(34) Bozkurt, A.; Meyer, W. H. *Solid State Ionics* **2001**, *138*, 259.
(35) Horng, J. C.; Raines, R. T. *Protein Sci.* **2006**, *15*, 74.
(36) Kakinoki, S.; Hirano, Y.; Oka, M. *Polym. Bull.* **2005**, *53*, 109.
(37) Chellgren, B. W.; Creamer, T. P. *Biochemistry* **2004**, *43*, 5864.

(38) Rucker, A. L.; Creamer, T. P. *Protein Sci.* **2002**, *11*, 980.
(39) Myer, Y. P.; Barnard, E. A. *Arch. Biochem. Biophys.* **1971**, *143*, 116.
(40) Peggion, E.; Cosani, A.; Terbojevich, M.; Scoffone, E. *Macromolecules* **1971**, *4*, 725.
(41) Colemann, M. M.; Graf, J. F.; Painter, P. C. *Specific Interactions and the Miscibility of Polymer Blends*; Technomic: Lancaster, PA, 1991.
(42) Berthomieu, C.; Dupeyrat, F.; Fontecave, M.; Verméglio, A.; Nivière, V. *Biochemistry* **2002**, *41*, 10360.
(43) Doyle, B. B.; Traub, W.; Lorenzi, G. P.; Blout, E. R. *Biochemistry* **1971**, *10*, 3052.
(44) Spezzacatena, C.; Perri, T.; Guantieri, V.; Sandberg, L. B.; Mitts, T. F.; Tamburro, A. M. *Eur. J. Org. Chem.* **2002**, *1*, 95.
(45) Ruokolainen, J.; Torkkeli, M.; Serimaa, R.; Komanschek, B. E.; Ikkala, O.; ten Brinke, G. *Phys. Rev. E* **1996**, *54*, 6646.
(46) Brewer, S. H.; Vu, D. M.; Tang, Y.; Li, Y.; Franzen, S.; Raleigh, D. P.; Dyer, R. B. *Proc. Natl. Acad. Sci. U.S.A.* **2005**, *102*, 16662.
(47) McCurdie, M. P.; Belfiore, L. A. *J. Polym. Sci., Part B: Polym. Phys.* **1999**, *37*, 301.
(48) Belfiore, L. A.; McCurdie, M. P. *Polym. Eng. Sci.* **2000**, *40*, 738.

BM7012845